

Research Article

Dynamical Analysis and Stabilizing Control of Inclined Rotational Translational Actuator Systems

Bingtuan Gao^{1,2} and Fei Ye¹

¹ School of Electrical Engineering, Southeast University, Nanjing 210096, China

² Jiangsu Key Laboratory of Smart Grid Technology and Equipment, Zhenjiang 212009, China

Correspondence should be addressed to Bingtuan Gao; gaobingtuan@seu.edu.cn

Received 5 March 2014; Revised 4 May 2014; Accepted 4 May 2014; Published 3 July 2014

Academic Editor: Reinaldo Martinez Palhares

Copyright © 2014 B. Gao and F. Ye. This is an open access article distributed under the Creative Commons Attribution License, which permits unrestricted use, distribution, and reproduction in any medium, provided the original work is properly cited.

Rotational translational actuator (RTAC) system, whose motions occur in horizontal planes, is a benchmark for studying of control techniques. This paper presents dynamical analysis and stabilizing control design for the RTAC system on a slope. Based on Lagrange equations, dynamics of the inclined RTAC system is achieved by selecting cart position and rotor angle as the general coordinates and torque acting on the rotor as general force. The analysis of equilibriums and their controllability yields that controllability of equilibriums depends on inclining direction of the inclined RTAC system. To stabilize the system to its controllable equilibriums, a proper control Lyapunov function including system energy, which is used to show the passivity property of the system, is designed. Consequently, a stabilizing controller is achieved directly based on the second Lyapunov stability theorem. Finally, numerical simulations are performed to verify the correctness and feasibility of our dynamical analysis and control design.

1. Introduction

Underactuated systems are a class of mechanical control systems whose control inputs are less than the number of configuration variables [1–3]. The RTAC system consisting of an unactuated translational oscillation cart and an actuated eccentric rotor attached to the cart is originally studied as a simplified model of a dual-spin spacecraft to investigate the resonance capture phenomenon [4]. Then, it is brought to us as a benchmark problem for nonlinear control by Bupp et al. [5]. The control objectives of RTAC system are to stabilize the translational position of the cart around its equilibrium and regulate the angular position of the rotor around one of its multiple equilibriums with the only control input torque acting on the rotor.

Stabilizing control design of RTAC has been extensively studied. Jankovic et al. [6] proposed cascade-based control designs for RTAC system. Bupp et al. [7] designed one integrator backstepping controller and three passive nonlinear controllers and implemented them on an experimental test bed of RTAC. Lee and Chang [8] proposed an adaptive backstepping control scheme based on a wavelet-based neural

network for RTAC system, and a compensated controller has been provided to enhance the control performance. Tsiotras et al. [9] applied the theory of L_2 disturbance attenuation for RTAC system. Petres et al. [10] employed RTAC to study the approximation and complexity tradeoff capabilities of the tensor product distributed compensation based control design. In [11], an equivalent-input-disturbance approach was developed to stabilize RTAC system with two steps based on the state variables of position. Moreover, in [12–14], controllers with only rotor angle feedback were designed for RTAC system. Most of the above results were based on simulation; however, approaches in [7, 8] had been validated through experimental results.

RTAC system considered in all the above mentioned papers is on horizontal planes; therefore, no gravity effect is considered in the dynamics and control design. Gao [15] considered dynamics and energy based control of a RTAC system with rotating motion appearing in a vertical plane, where gravity affecting the rotor motion has to be included. Avis et al. [16] presented an energy-based and entropy-based hybrid control framework to stabilize RTAC system with rotating motion in a vertical plane and compared the two controllers'

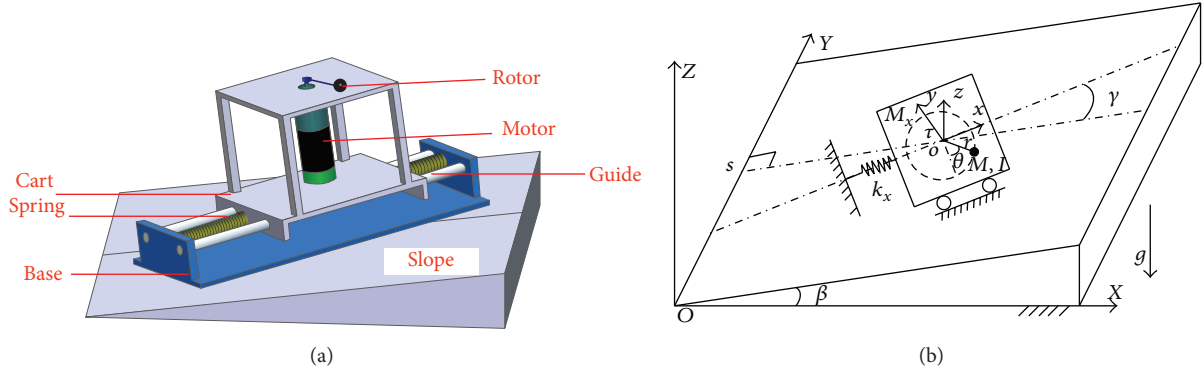


FIGURE 1: The inclined RTAC system.

performance with experiments. However, it should be noted that, in real applications, absolute horizontal or vertical plane does not exist. In other words, the motions of RTAC system will be in inclined planes because of the assembly or inherent unlevel installation plane. In this paper, dynamical modeling and equilibriums' controllability of inclined RTAC systems will be analyzed in detail. And according to the passivity of the system, an energy-based control technique [15, 17–20] is employed to design a simple PD (proportional derivative) controller for the inclined RTAC system.

The rest of paper is organized as follows. Dynamics of the inclined RTAC is developed according to Lagrange equations in Section 2. Based on the developed dynamics, its equilibriums and their controllability conditions are analyzed in Section 3. After that, a proper Lyapunov function including system energy is designed to generate a simple controller for the system in Section 4. Simulation results and discussions are provided in Section 5. And conclusions are summarized in the last section.

2. Dynamics

According to the benchmark system RTAC on the horizontal plane, inclined RTAC system is depicted as in Figure 1. A coordinate frame $oxyz$ is attached to the base of the RTAC system, with the origin at the center of the cart when the spring is with free status. The x -axis is along the translational movement of the cart, and the z -axis is perpendicular to the base plane of the RTAC system. According to the definition of $oxyz$, another world frame $OXYZ$ is defined, as shown in Figure 1, for the slope on which the RTAC system locates. The motions of RTAC system occur in the inclined plane oxy having an angle β with respect to the horizontal plane OXY , and inclining direction of the RTAC system is denoted with γ as shown in Figure 1. Parameters of the inclined RTAC system are defined similarly as in [5] according to the coordinate frame $oxyz$. The cart of mass M_x is connected to a fixed base by a linear spring of stiffness k_x . The cart is constrained to have one-dimensional translational motion with x denoting the travel distance. The actuated rotor attached to the cart has mass m and moment of inertia I about its center of mass, and the eccentric distance of the rotor is r . Control input torque applied to the rotor is denoted by τ . Let x and \dot{x} denote

the translational position and velocity of the cart, respectively, and let θ and $\dot{\theta}$ denote angular position and its velocity of the rotor rotating away from the negative y -axis, respectively. Since the gravitational force has to be considered for the inclined RTAC system, let g be the gravity constant.

The total kinetic energy T of the system is the sum of kinetic energy T_x , corresponding to the equivalent mass of translational cart and kinetic energy T_m of the rotational rotor:

$$\begin{aligned} T &= T_x + T_m \\ &= \frac{1}{2} (M_x + m) \dot{x}^2 + mr \cos \theta \dot{\theta} + \frac{1}{2} (mr^2 + I) \dot{\theta}^2. \end{aligned} \quad (1)$$

To calculate the potential energy of the system, let zero potential energy of the gravity be the center of the cart when the spring is with free status, that is, the origin of the coordinates frame $oxyz$. According to Figure 1, the mass points of cart o_1 and rotor A on the slope can be depicted as in Figure 2, where $ol \perp os$, $o_1l_1 \parallel ol$, $F_1o_1F_2 \parallel os$, and a is the projection of point A on line os . The planar coordinates oxy are extracted from the coordinates frame $oxyz$ in Figure 1. The circle with center o_1 and radius r denotes the rotating trajectory of the rotor. Because, at point o , the system has zero potential energy both for the spring and the gravity, the total potential energy, which is the sum of the potential energy P_s corresponding to the spring and potential energy P_g corresponding to the gravity, can be calculated as

$$\begin{aligned} P &= P_s + P_g \\ &= \frac{1}{2} k_x x^2 - M_x g |op| \sin \beta + mg |oa| \sin \beta \\ &= \frac{1}{2} k_x x^2 + (M_x + m) gx \cos \gamma \sin \beta \\ &\quad + mgr \sin (\gamma + \theta) \sin \beta, \end{aligned} \quad (2)$$

where $|\cdot|$ means the length of the line segment.

Therefore, the Lagrangian L can be calculated as

$$L = T - P. \quad (3)$$

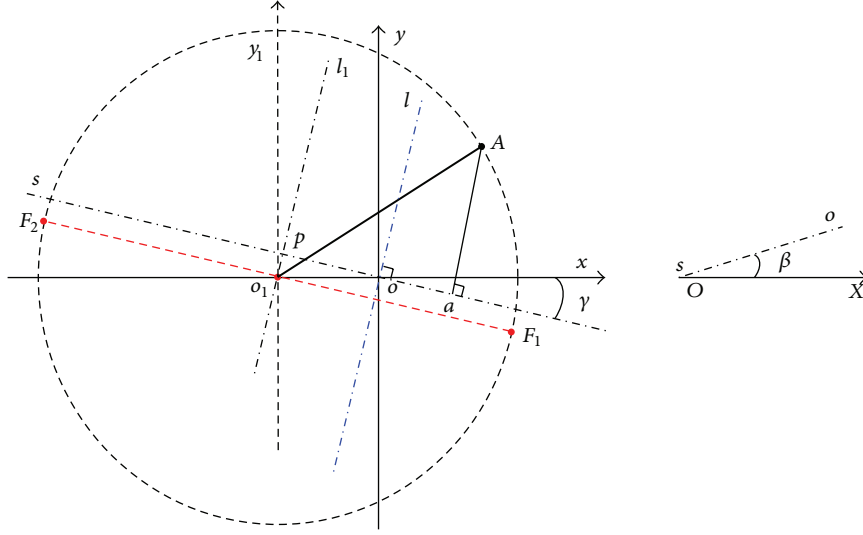


FIGURE 2: Mass points analysis of the inclined RTAC system.

By choosing x and θ as the generalized coordinates and τ as the generalized force, the Lagrange equations of motion for the inclined RTAC system are as follows:

$$\frac{d}{dt} \left(\frac{\partial L}{\partial \dot{x}} \right) - \frac{\partial L}{\partial x} = -N_x \quad (4)$$

$$\frac{d}{dt} \left(\frac{\partial L}{\partial \dot{\theta}} \right) - \frac{\partial L}{\partial \theta} = \tau - N_r, \quad (5)$$

where N_x and N_r denote the disturbance inputs acting on the translational moving cart and rotating rotor, respectively. Dynamics of the system can be calculated as

$$(M_x + m) \ddot{x} + mr \cos \theta \ddot{\theta} - mr \sin \theta \dot{\theta}^2 + k_x x + (M_x + m) g \cos \gamma \sin \beta + N_x = 0 \quad (6)$$

$$mr \cos \theta \ddot{x} + (mr^2 + I) \ddot{\theta} + mgr \cos (\gamma + \theta) \sin \beta + N_r = \tau. \quad (7)$$

By choosing the variable vector $\mathbf{q} = (x, \theta)$, the above two equations can be written in a compact form as follows:

$$\mathbf{M}(\mathbf{q}) \ddot{\mathbf{q}} + \mathbf{C}(\mathbf{q}, \dot{\mathbf{q}}) \dot{\mathbf{q}} + \mathbf{G}(\mathbf{q}) + \mathbf{N} = \mathbf{U}, \quad (8)$$

where $\mathbf{M}(\mathbf{q})$, $\mathbf{C}(\mathbf{q}, \dot{\mathbf{q}})$, $\mathbf{G}(\mathbf{q})$, \mathbf{N} , and \mathbf{U} represent inertia matrix, Coriolis and centrifugal force matrix, potential matrix,

disturbance force vector, and control input vector of the inclined RTAC system, respectively,

$$\begin{aligned} \mathbf{M}(\mathbf{q}) &= \begin{bmatrix} M_x + m & mr \cos \theta \\ mr \cos \theta & mr^2 + I \end{bmatrix}, \\ \mathbf{C}(\mathbf{q}, \dot{\mathbf{q}}) &= \begin{bmatrix} 0 & -mr \dot{\theta} \sin \theta \\ 0 & 0 \end{bmatrix}, \\ \mathbf{G}(\mathbf{q}) &= \begin{bmatrix} k_x x + (M_x + m) g \cos \gamma \sin \beta \\ mgr \cos (\gamma + \theta) \sin \beta \end{bmatrix}, \\ \mathbf{N} &= \begin{bmatrix} N_x \\ N_r \end{bmatrix}, \quad \mathbf{U} = \begin{bmatrix} 0 \\ \tau \end{bmatrix}. \end{aligned} \quad (9)$$

Remark 1. It can be observed straightforwardly from dynamics (8) that θ is the actuated variable and x is the unactuated variable in the configuration variable vector \mathbf{q} . Because the unactuated variable x has to be stabilized around its equilibrium and actuated variable θ has to be regulated around one of its equilibriums with the only control input τ , the inclined RTAC system is an underactuated system.

Remark 2. The inclined angle β of the system could be caused by assembly or unlevel installation plane. Without loss of generality, it can be defined as $\beta \in [0^\circ, 90^\circ]$. However, the angle γ denoting inclining direction of the system could be arbitrary. Therefore, it can be selected as $\gamma \in [0^\circ, 360^\circ]$.

Remark 3. When the inclined angle β is zero, that is, the RTAC system on a horizontal plane, dynamics of inclined RTAC system (8) can be deduced as (neglecting the friction torque of rotor N_r)

$$\begin{aligned} (M_x + m) \ddot{x} + mr \cos \theta \ddot{\theta} - mr \sin \theta \dot{\theta}^2 + k_x x &= -N_x \\ mr \cos \theta \ddot{x} + (mr^2 + I) \ddot{\theta} &= \tau \end{aligned} \quad (10)$$

which is the same as the dynamics of RTAC system provided in [5].

3. Analysis of Controllable Equilibriums

To derive the equilibriums of the system, we neglect the disturbance force matrix \mathbf{N} in the dynamics of the inclined RTAC system. By choosing the system state $\mathbf{x} = (x_1, x_2, x_3, x_4) = (x, \dot{x}, \theta, \dot{\theta})$ and system input $u = \tau$, the dynamics (8) can be rewritten in general affine form as follows:

$$\dot{\mathbf{x}} = \mathbf{f}(\mathbf{x}) + \mathbf{g}(\mathbf{x})u, \quad (11)$$

where

$$\mathbf{f}(\mathbf{x}) = \begin{bmatrix} x_2 \\ \frac{f_2}{\det(\mathbf{M})} \\ x_4 \\ \frac{f_4}{\det(\mathbf{M})} \end{bmatrix}, \quad \mathbf{g}(\mathbf{x}) = \begin{bmatrix} 0 \\ \frac{-b \cos x_3}{\det(\mathbf{M})} \\ 0 \\ \frac{a}{\det(\mathbf{M})} \end{bmatrix}$$

$$f_2 = (b \sin x_3 x_4^2 - k_x x_1 - ag \cos \gamma \sin \beta) c$$

$$+ b^2 g \cos x_3 \cos(\gamma + x_3) \sin \beta \quad (12)$$

$$f_4 = -b \cos x_3 (b \sin x_3 x_4^2 - k_x x_1 - ag \cos \gamma \sin \beta)$$

$$- abg \cos(\gamma + x_3) \sin \beta$$

$$\det(\mathbf{M}) = (M_x + m)I + M_x m r^2$$

$$+ m^2 r^2 \sin^2 x_3 > 0$$

$$a = M_x + m, \quad b = mr, \quad c = mr^2 + I.$$

To solve the equilibriums of the unforced system, let $u = 0$ and $\dot{\mathbf{x}} = 0$. Therefore, we have $x_2 = x_4 = 0$ and $f_2 = f_4 = 0$ which can be expressed as

$$(-k_x x_1 - ag \cos \gamma \sin \beta) c$$

$$+ b^2 g \cos x_3 \cos(\gamma + x_3) \sin \beta = 0 \quad (13)$$

$$-b \cos x_3 (-k_x x_1 - ag \cos \gamma \sin \beta)$$

$$- abg \cos(\gamma + x_3) \sin \beta = 0. \quad (14)$$

Simplifying the above two equations by considering that all the parameters k_x, a, b, c , and g are positive, we have

$$\det(\mathbf{M}) b g \cos(\gamma + x_3) \sin \beta = 0. \quad (15)$$

Notice that $\det(\mathbf{M})$ is also positive. When the inclined angle $\beta = 0$, the equilibrium of the rotor angle cannot be decided based on (15); that is, x_3 is an arbitrary angle. When $\beta \in (0, 90]$, the equilibrium of x_3 can be calculated as

$$x_3 = \theta_e = \left(\frac{2k+1}{2} \right) \pi - \gamma, \quad k = 0, \pm 1, \pm 2, \dots \quad (16)$$

Therefore, the equilibrium of the rotor angle θ_e can be expressed as

$$x_3 = \theta_e, \quad \beta = 0$$

$$x_3 = \theta_e = \left(\frac{2k+1}{2} \right) \pi - \gamma, \quad k = 0, \pm 1, \pm 2, \dots, \quad 0 < \beta \leq 90 \quad (17)$$

Substituting (15) into (13), the equilibrium of the cart position x_e can be calculated as

$$x_1 = x_e = -\frac{ag \cos \gamma \sin \beta}{k_x}. \quad (18)$$

As a result, the equilibriums of the inclined RTAC system can be achieved by combining (18) and (17):

$$\mathbf{x}_e = \left[\frac{-ag \cos \gamma \sin \beta}{k_x}, 0, \left(\frac{2k+1}{2} \right) \pi - \gamma, 0 \right], \quad (19)$$

$$k = 0, \pm 1, \pm 2, \dots$$

Remark 4. When RTAC system is on a horizontal plane without gravity affecting it, equilibriums of the benchmark system are stable. However, the inclined RTAC system, similar to pendulum-like systems, has two types of equilibriums, that is, up equilibriums with high potential energy of gravity and down equilibriums with low potential energy of gravity. The up equilibriums are

$$\mathbf{x}_{e,\text{up}} = \left[\frac{-ag \cos \gamma \sin \beta}{k_x}, 0, \left(\frac{4k+1}{2} \right) \pi - \gamma, 0 \right], \quad (20)$$

where the potential energy of gravity is $-(1/2)a^2 g^2 \cos^2 \gamma \sin^2 \beta + mgr \sin \beta$. And the up equilibriums are self-unstable which are not interesting in this paper. The down equilibriums are

$$\mathbf{x}_{e,\text{down}} = \left[\frac{-ag \cos \gamma \sin \beta}{k_x}, 0, \left(\frac{4k+3}{2} \right) \pi - \gamma, 0 \right], \quad (21)$$

where the potential energy of gravity is $-(1/2)a^2 g^2 \cos^2 \gamma \sin^2 \beta - mgr \sin \beta$. In the next section, we will develop a simple linear controller for the inclined RTAC system to its typical down equilibrium from any initial conditions.

To analyze controllability around equilibriums (19), we can check if the following matrix is full rank:

$$\mathbf{C} = [\mathbf{B}, \mathbf{A}\mathbf{B}, \mathbf{A}^2\mathbf{B}, \mathbf{A}^3\mathbf{B}], \quad (22)$$

where

$$\mathbf{A} := \left(\frac{\partial}{\partial \mathbf{x}} \right) \mathbf{f}(\mathbf{x}_e), \quad (23)$$

$$\mathbf{B} := \mathbf{g}(\mathbf{x}_e).$$

Calculating **A**, **B**, and **C**, we can get

$$\mathbf{A} = \begin{bmatrix} 0 & 1 & 0 & 0 \\ a_{21} & 0 & a_{23} & 0 \\ 0 & 0 & 1 & 0 \\ a_{41} & 0 & a_{43} & 0 \end{bmatrix}, \quad \mathbf{B} = \begin{bmatrix} 0 \\ b_2 \\ 0 \\ b_4 \end{bmatrix}, \quad (24)$$

$$\mathbf{C} = \begin{bmatrix} 0 & b_2 & 0 & a_{21}b_2 + a_{23}b_4 \\ b_2 & 0 & a_{21}b_2 + a_{23}b_4 & 0 \\ 0 & b_4 & 0 & a_{41}b_2 + a_{43}b_4 \\ b_4 & 0 & a_{41}b_2 + a_{43}b_4 & 0 \end{bmatrix},$$

where

$$\begin{aligned} a_{21} &= -ck_x[\det(\mathbf{M})]^{-1}, \\ a_{23} &= -b^2g \sin(2\theta_e + \gamma) \sin \beta [\det(\mathbf{M})]^{-1}, \\ a_{41} &= b \cos \theta_e k_x [\det(\mathbf{M})]^{-1}, \\ a_{43} &= abg \cos \theta_e \sin \gamma \sin \beta [\det(\mathbf{M})]^{-1}, \\ b_2 &= -b \cos \theta_e [\det(\mathbf{M})]^{-1}, \\ b_4 &= a [\det(\mathbf{M})]^{-1}. \end{aligned} \quad (25)$$

To check the full rank condition of matrix **C**, one can calculate its determination as follows:

$$\det(\mathbf{C}) = \begin{vmatrix} b_2 & a_{21}b_2 + a_{23}b_4 & 0 & 0 \\ b_4 & a_{41}b_2 + a_{43}b_4 & 0 & 0 \\ 0 & 0 & b_2 & a_{21}b_2 + a_{23}b_4 \\ 0 & 0 & b_4 & a_{41}b_2 + a_{43}b_4 \end{vmatrix} \quad (26)$$

$$= \begin{vmatrix} \mathbf{C}'_{2 \times 2} & \mathbf{0}_{2 \times 2} \\ \mathbf{0}_{2 \times 2} & \mathbf{C}'_{2 \times 2} \end{vmatrix}.$$

Therefore, one can calculate the determination $\det(\mathbf{C}') \neq 0$ to find out full rank conditions of itself and **C** as follows:

$$\det(\mathbf{C}') = \frac{b \cos \theta_e}{[\det(\mathbf{M})]^3} \times [-k_x (ac - b^2 \cos^2 \theta_e) + a^2 bg \sin \theta_e \cos \gamma \sin \beta]. \quad (27)$$

In the following, we discuss three cases to obtain the conditions on full rank of matrix **C**.

Case 1. $\beta = 0$; that is, the RTAC system is on the horizontal plane.

Substituting the parameters a, b, c into (27), determination of matrix **C'** becomes

$$\det(\mathbf{C}') = \frac{-mrk_x \cos \theta_e}{[\det(\mathbf{M})]^2}, \quad (28)$$

where $m, r, k_x, \det(\mathbf{M})$ are all positive parameters. Therefore, the full rank constrain for matrix **C'** (also matrix **C**) will be $\cos \theta_e \neq 0$; that is,

$$\theta_e \neq \frac{2k+1}{2}\pi, \quad k = 0, \pm 1, \pm 2, \dots \quad (29)$$

It can be observed from condition (29) that the equilibriums will be uncontrollable once the rotor angles are aligned to the moving direction of the translational cart.

Case 2. $0 < \beta \leq 90^\circ$ and $\theta_e = (2k+1.5)\pi - \gamma$, that is, the down stable equilibriums (21) of the inclined RTAC system.

Calculating the determination of matrix **C'** similarly renders

$$\begin{aligned} \det(\mathbf{C}') &= \frac{-mr \cos \theta_e}{[\det(\mathbf{M})]^3} \\ &\times [k_x \cdot \det(\mathbf{M}) + (M_x + m)^2 mrg \sin^2 \theta_e \sin \beta] \\ &= \frac{mr \sin \gamma}{[\det(\mathbf{M})]^3} \\ &\times [k_x \cdot \det(\mathbf{M}) + (M_x + m)^2 mrg \cos^2 \gamma \sin \beta], \end{aligned} \quad (30)$$

where $M_x, m, r, k_x, g, \det(\mathbf{M}), \sin \beta$ are all positive parameters. Therefore, for the down stable equilibriums of the inclined RTAC system, the controllability condition becomes

$$\gamma \neq k\pi, \quad k = 0, \pm 1, \pm 2, \dots \quad (31)$$

According to the relationship between θ and γ that $\theta_e = (2k+1.5)\pi - \gamma$, for the down stable equilibriums of the inclined RTAC system, controllability condition (31) still implies that the equilibriums are uncontrollable when the rotor angles are aligned to the moving direction of the translational cart.

Case 3. $0 < \beta \leq 90^\circ$ and $\theta_e = (2k+0.5)\pi - \gamma$, that is, the up unstable equilibriums of the inclined RTAC system.

Calculating determination of matrix **C'** becomes as follows:

$$\begin{aligned} \det(\mathbf{C}') &= \frac{mr \cos \theta_e}{[\det(\mathbf{M})]^3} \\ &\times [-k_x \cdot \det(\mathbf{M}) + (M_x + m)^2 mrg \sin^2 \theta_e \sin \beta] \\ &= \frac{mr \sin \gamma}{[\det(\mathbf{M})]^3} \\ &\times [-k_x \cdot \det(\mathbf{M}) + (M_x + m)^2 mrg \cos^2 \gamma \sin \beta]. \end{aligned} \quad (32)$$

Therefore, controllable conditions for the up unstable equilibriums of the inclined RTAC system on slopes are as follows:

$$\sin \gamma \neq 0, \quad (33)$$

$$\begin{aligned} &[(M_x + m)^2 mrg \sin \beta - m^2 r^2 k_x] \cos^2 \gamma \\ &\neq (M_x I + mI + Mmr^2) k_x. \end{aligned} \quad (34)$$

Comparing controllability conditions on the two cases of inclined RTAC system, they have the same controllable equilibriums. To meet the condition (34) for up unstable equilibriums, proper physical parameters of the inclined

RTAC system can be considered when inclining parameters β, γ are fixed. Since the up unstable equilibriums are not interesting, condition (34) will not be studied in detail in this paper.

Remark 5. It is straightforward that the actuated variable θ can be controlled directly by the input torque τ ; however, the unactuated cart motion must be controlled through dynamical coupling of the system. The controllable equilibriums for the (horizontal or inclined) RTAC system can be explained based on (7) intuitively: the acceleration \ddot{x} of cart's translational motion is controlled by input torque τ with a coupling coefficient related to $\cos \theta$. If we set θ_e to $((2k + 1)/2)\pi$, rotor angle can always be brought to $((2k + 1)/2)\pi$ with a simple controller. Consequently, we have $\cos \theta = 0$, which means that the coupling item from input torque used to control cart motion will disappear. In other words, the input control torque τ will lose control of the cart position x as soon as the rotor angle θ is brought to $((2k + 1)/2)\pi$. Therefore, the RTAC systems are uncontrollable when the desired rotor angles are aligned to the moving direction of the translational cart.

4. Energy Based Control Design

In this section, energy is employed to derive the passivity of the inclined RTAC system. Based on the passivity property, a simple PD controller is achieved for the inclined system to its controllable equilibriums from initial conditions.

Overall energy of the inclined RTAC system can be calculated with

$$\begin{aligned} E &= T + P \\ &= \frac{1}{2} \dot{\mathbf{q}}^T \mathbf{M}(\mathbf{q}) \dot{\mathbf{q}} + P \\ &= \frac{1}{2} \dot{\mathbf{q}}^T \mathbf{M}(\mathbf{q}) \dot{\mathbf{q}} + \frac{1}{2} k_x x^2 + (M_x + m) g x \cos \gamma \sin \beta \\ &\quad + mgr \sin(\gamma + \theta) \sin \beta. \end{aligned} \quad (35)$$

Differentiating E , we can get

$$\begin{aligned} \dot{E} &= \dot{\mathbf{q}}^T \mathbf{M}(\mathbf{q}) \ddot{\mathbf{q}} + \frac{1}{2} \dot{\mathbf{q}}^T \dot{\mathbf{M}}(\mathbf{q}) \dot{\mathbf{q}} + \dot{\mathbf{q}}^T \mathbf{G}(\mathbf{q}) \\ &= \dot{\mathbf{q}}^T \left[-\mathbf{C}(\mathbf{q}, \dot{\mathbf{q}}) \dot{\mathbf{q}} - \mathbf{G}(\mathbf{q}) + \mathbf{U} + \frac{1}{2} \dot{\mathbf{M}}(\mathbf{q}) \dot{\mathbf{q}} \right] + \dot{\mathbf{q}}^T \mathbf{G}(\mathbf{q}) \\ &= \dot{\mathbf{q}}^T \mathbf{U} = \dot{\theta} \tau. \end{aligned} \quad (36)$$

Integrating both sides of (36), we have

$$\int_0^t \dot{\theta}(\tau) \tau d\tau = E(t) - E(0) \geq -E(0). \quad (37)$$

Therefore, based on the definition of passivity [3], the system having τ as input and $\dot{\theta}$ as output is passive.

TABLE 1: Simulation parameters.

Parameter (Units)	Value	Description
M_x (kg)	1.3608	Cart mass of axis x
m (kg)	0.096	Rotor mass
k_x (N/m)	186.3	Spring stiffness of axis x
r (m)	0.0592	Eccentric distance of rotor
I (kg·m ²)	0.0002175	Rotor inertia

According to the derived passivity property of the inclined RTAC system, a control Lyapunov function candidate including system energy E is designed as

$$V = k_1 (E - E_0) + \frac{k_2}{2} (\theta - \theta_0)^2, \quad (38)$$

where $k_1 > 0$, $k_2 > 0$, and

$$\begin{aligned} E_0 &= -\frac{1}{2} k_x^{-1} (M_x + m)^2 g^2 \cos^2 \gamma \sin^2 \beta - mgr \sin \beta \\ \theta_0 &= k\pi + \frac{3}{2}\pi - \gamma \end{aligned} \quad (39)$$

are potential energy and rotor angle (here we choose $\theta_0 \in (-\pi, \pi]$) at the down stable equilibrium, respectively. Because the smallest system energy is E_0 , the designed Lyapunov function (38) is positive definite.

Differentiating V , we have

$$\dot{V}(q, \dot{q}) = k_1 \dot{E} + k_2 (\theta - \theta_0) \dot{\theta} = \dot{\theta} [k_1 \tau + k_2 (\theta - \theta_0)]. \quad (40)$$

According to the second Lyapunov stability theorem, the controller should guarantee the negative defined \dot{V} . By choosing

$$k_1 \tau + k_2 (\theta - \theta_0) = -k_3 \dot{\theta}, \quad (41)$$

where $k_3 > 0$, we get

$$\dot{V}(q, \dot{q}) = -k_3 \dot{\theta}^2. \quad (42)$$

Therefore, a simple PD controller for the inclined RTAC system is derived as

$$\tau = -\frac{1}{k_1} [k_2 (\theta - \theta_0) + k_3 \dot{\theta}]. \quad (43)$$

Finally, by using LaSalle's stability theorem [3], the global asymptotic stability of the closed-loop system consisting of dynamics (8) and controller (43) can be concluded.

5. Simulations

In order to verify the dynamical analysis and control design for the inclined RTAC system, simulations were programmed and performed with Matlab/Simulink. Following [5], the physical parameters of the inclined RTAC system are chosen as shown in Table 1.

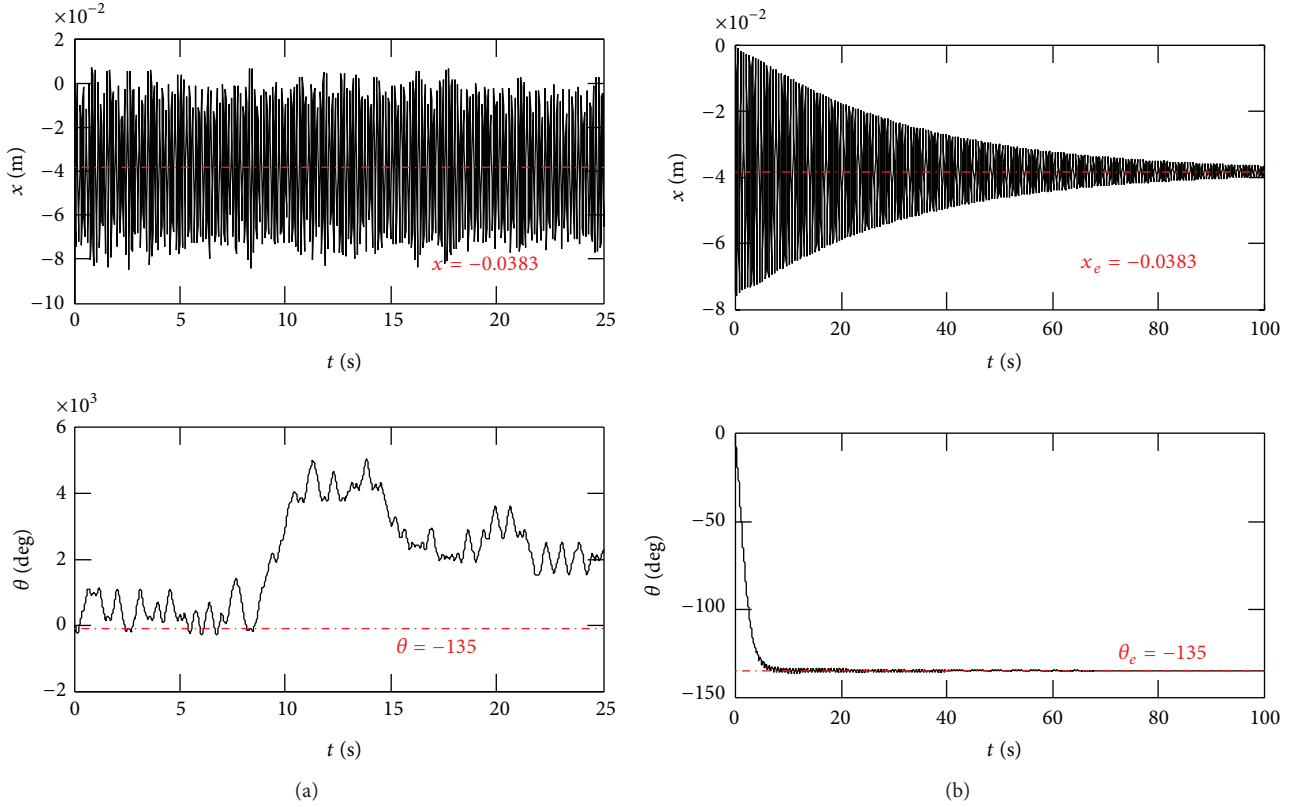


FIGURE 3: Simulation results on dynamics: $\mathbf{x}(0) = (0, 0, 0, 0)$, $\tau = 0$, and $\gamma = \beta = 45^\circ$; left column: no friction; right column: friction coefficients, $d_x = 0.05$, $d_r = 0.03$.

Figure 3 shows the simulation results to verify the system dynamics (8) and its equilibriums (19), where the left column is without friction and the right column is with friction. In the simulations, the initial conditions of the system are selected as $(x, \dot{x}, \theta, \dot{\theta}) = (0, 0, 0, 0)$, $\tau = 0$, and $\gamma = \beta = 45^\circ$ which guarantees that the equilibriums are controllable according to (31) and the disturbance friction forces are modeled as $N_x = d_x \dot{x}$ and $N_r = d_r \dot{\theta}$, where d_x, d_r are the friction constants and are set as $d_x = 0.005$ and $d_r = 0.03$. For the inclined RTAC system without disturbances, whose simulation results are shown as left column of Figure 3, cart oscillates along x -axis about its equilibrium (18); however, the trajectory of rotor angle θ is a combination of rounds of rotation and oscillation within one round, which can be imaged because of period feature of its equilibrium (17). Once frictions are injected into the system, simulation results being shown as right column of Figure 3, both cart position and rotor angle will damp to their equilibriums: cart motion of x -axis is damped oscillations with respect to its equilibrium $x = -0.0383$ m, and the rotor angle will be stuck to $\theta = -135^\circ$, one of its equilibriums, and damped quickly under friction.

Figure 4 shows the simulation results to illustrate the performance of the closed-loop control system consisting of system dynamics (8) and designed controller (43). Initial conditions for the simulation are $(x, \dot{x}, \theta, \dot{\theta}) = (0, 0, 0, 0)$, $\gamma = \beta = 45^\circ$, and $d_x = d_r = 0$. Parameters of the controller are

selected as $k_1 = 440$, $k_2 = 5.4$, and $k_3 = 1$. As one can see from the simulation results shown in Figure 4, the designed PD controller (43) can bring the states of inclined RTAC system from $(0, 0, 0, 0)$ to its equilibrium $(-0.0383, 0, 225, 0)$ in 30 s. And the stabilized rotor angle 225° here has a 360° difference compared to the rotor angle -135° as shown in Figure 3, which means the same rotor position in real physical system. From Figure 4, one also can observe that the system energy will be brought to -0.1761 J which is the lowest level. During the stabilizing process, the peak value of control torque is no more than 0.05 Nm, and the continuous control torque is no more than 0.02 Nm.

To validate the controllable condition (31) of down equilibriums of the inclined RTAC system, performance of the close-loop control system consisting of system dynamics (8) and designed controller (43) under the same initial conditions and controller parameters other than $\gamma = 0$ is simulated and shown as Figure 5. The condition $\gamma = 0$ which leads to the equilibrium of the rotor angle is aligned to the moving direction of the cart, which violates the controllable condition (31). One can see that the rotor angle is stabilized by the same controller in 5 s; however, the cart position is out of control and oscillates about its equilibrium -0.0542 m. Once the rotor angle is stabilized, the control output τ becomes zero, and system energy is about -0.1 J which is much higher than the lowest potential energy -0.3192 J.

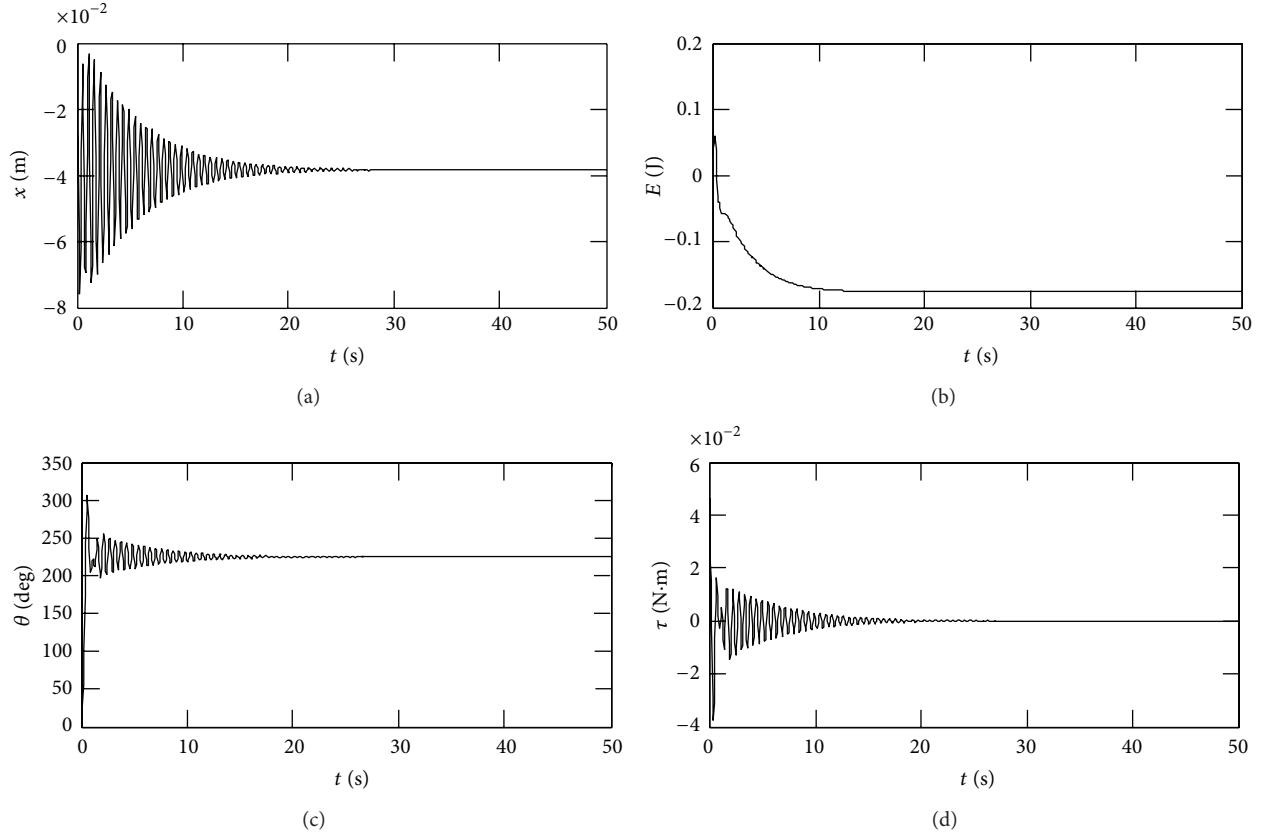


FIGURE 4: Simulation results on closed-loop control system: $\mathbf{x}(0) = (0, 0, 0, 0)$, $\gamma = \beta = 45$, $d_x = d_r = 0$, $k_1 = 440$, $k_2 = 5.4$, and $k_3 = 1$.

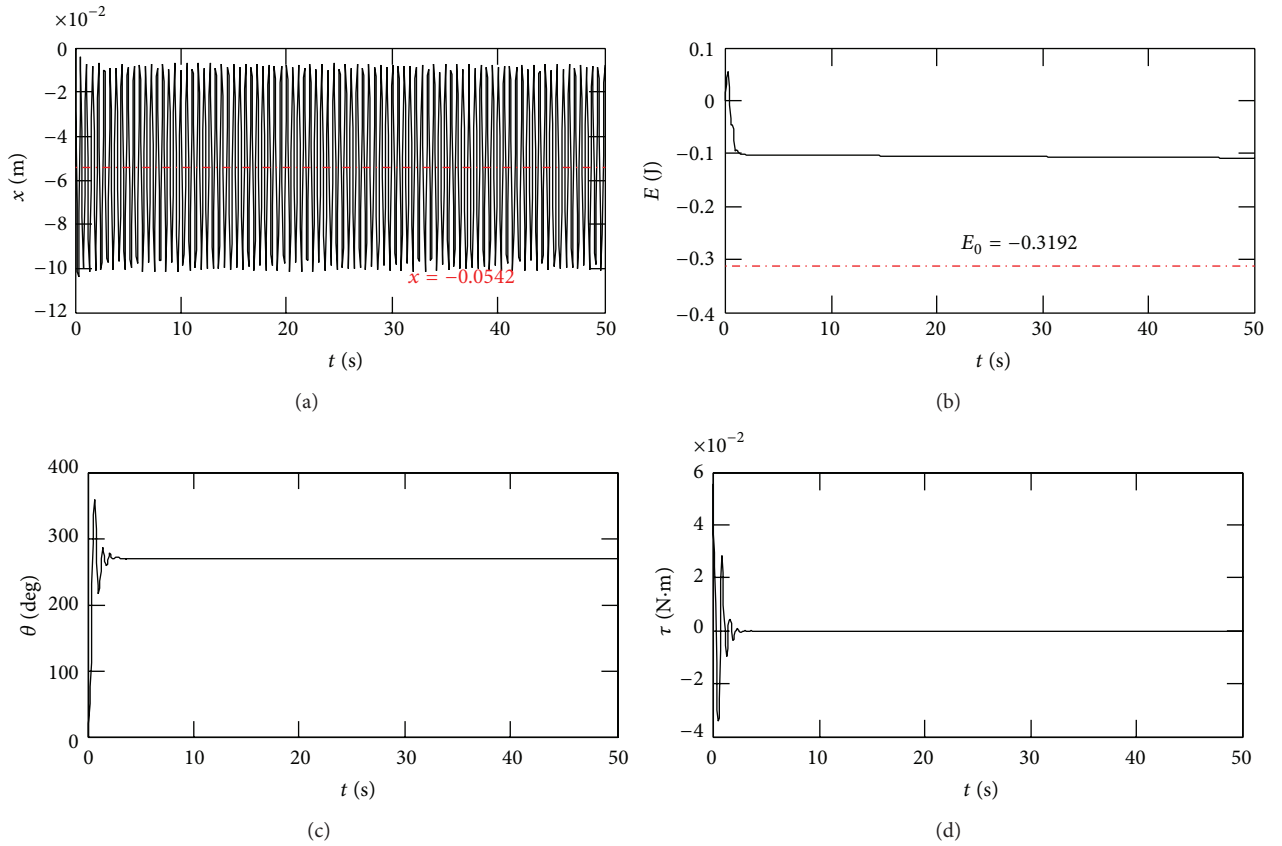


FIGURE 5: Simulation results on closed-loop control system: $\mathbf{x}(0) = (0, 0, 0, 0)$, $\gamma = 0$, $\beta = 45$, $d_x = d_r = 0$, $k_1 = 440$, $k_2 = 5.4$, and $k_3 = 1$.

As a result, three sets of simulation results validate the dynamical analysis and control design for the inclined RTAC system in the previous sections.

6. Conclusion

Due to the assembly or unlevelled installation base, RTAC system cannot be on an absolute horizontal plane, which is used as a benchmark for evaluating nonlinear design techniques. This paper extends the standardized RTAC system to a more general case, that is, inclined RTAC system. Detailed dynamical modeling and analysis on equilibriums show that the down stable equilibriums are controllable when the inclined direction is not aligned to the oscillating direction of the cart. And a simple PD controller was developed based on passivity of the system. Simulation results verified the correctness and feasibility of the dynamical analysis and control design for the inclined RTAC system. The dynamical analyzing result and designed controller for the inclined RTAC system can be reduced and applied to the benchmark RTAC system.

Conflict of Interests

The authors declare that there is no conflict of interests regarding the publication of this paper.

Acknowledgments

This work is financially supported by the National Science Foundation of China (NSFC) under no. 11102039 and the Natural Science Foundation of Jiangsu Province under no. BK2011456.

References

- [1] M. W. Spong, "Underactuated mechanical systems," in *Control Problems in Robotics and Automation*, B. Siciliano and K. P. Valavanis, Eds., pp. 135–150, Springer, London, UK, 1998.
- [2] M. Reyhanoglu, A. van der Schaft, N. H. McClamroch, and I. Kolmanovsky, "Dynamics and control of a class of underactuated mechanical systems," *IEEE Transactions on Automatic Control*, vol. 44, no. 9, pp. 1663–1671, 1999.
- [3] I. Fantoni and R. Lozano, *Nonlinear Control for Underactuated Mechanical Systems*, Springer, London, UK, 2002.
- [4] C.-J. Wan, D. S. Bernstein, and V. T. Coppola, "Global stabilization of the oscillating eccentric rotor," *Nonlinear Dynamics*, vol. 10, no. 1, pp. 49–62, 1996.
- [5] R. T. Bupp, D. S. Bernstein, and V. T. Coppola, "A benchmark problem for nonlinear control design," *International Journal of Robust and Nonlinear Control*, vol. 8, no. 4-5, pp. 307–310, 1998.
- [6] M. Jankovic, D. Fontaine, and P. V. Kokotović, "TORA example: cascade- and passivity-based control designs," *IEEE Transactions on Control Systems Technology*, vol. 4, no. 3, pp. 292–297, 1996.
- [7] R. T. Bupp, D. S. Bernstein, and V. T. Coppola, "Experimental implementation of integrator backstepping and passive nonlinear controllers on the RTAC testbed," *International Journal of Robust and Nonlinear Control*, vol. 8, no. 4-5, pp. 435–457, 1998.
- [8] C.-H. Lee and S.-K. Chang, "Experimental implementation of nonlinear TORA system and adaptive backstepping controller design," *Neural Computing and Applications*, vol. 21, no. 4, pp. 785–800, 2012.
- [9] P. Tsiotras, M. Corless, and M. A. Rotea, "An L_2 disturbance attenuation solution to the nonlinear benchmark problem," *International Journal of Robust and Nonlinear Control*, vol. 8, no. 4-5, pp. 311–330, 1998.
- [10] Z. Petres, P. Baranyi, and H. Hashimoto, "Approximation and complexity trade-off by TP model transformation in controller design: a case study of the TORA system," *Asian Journal of Control*, vol. 12, no. 5, pp. 575–585, 2010.
- [11] J. She, A. Zhang, X. Lai, and M. Wu, "Global stabilization of 2-DOF underactuated mechanical systems—an equivalent-input-disturbance approach," *Nonlinear Dynamics*, vol. 69, no. 1-2, pp. 495–509, 2012.
- [12] T. Burg and D. Dawson, "Additional notes on the TORA example: a filtering approach to eliminate velocity measurements," *IEEE Transactions on Control Systems Technology*, vol. 5, no. 5, pp. 520–523, 1997.
- [13] G. Escobar, R. Ortega, and H. Sira-Ramírez, "Output-feedback global stabilization of a nonlinear benchmark system using a saturated passivity-based controller," *IEEE Transactions on Control Systems Technology*, vol. 7, no. 2, pp. 289–293, 1999.
- [14] F. Celani, "Output regulation for the TORA benchmark via rotational position feedback," *Automatica*, vol. 47, no. 3, pp. 584–590, 2011.
- [15] B. T. Gao, "Dynamical modeling and energy-based control design for TORA," *Acta Automatica Sinica*, vol. 34, no. 9, pp. 1221–1224, 2008.
- [16] J. M. Avis, S. G. Nersisov, R. a. . Nathan, and K. R. Muske, "A comparison study of nonlinear control techniques for the RTAC system," *Nonlinear Analysis*, vol. 11, no. 4, pp. 2647–2658, 2010.
- [17] B. Gao, X. Zhang, H. Chen, and J. Zhao, "Energy-based control design of an underactuated 2-dimensional TORA system," in *Proceedings of the IEEE/RSJ International Conference on Intelligent Robots and Systems (IROS '09)*, pp. 1296–1301, St. Louis, Mo, USA, October 2009.
- [18] B. Gao, J. Xu, J. Zhao, and X. Huang, "Stabilizing control of an underactuated 2-dimensional tora with only rotor angle measurement," *Asian Journal of Control*, vol. 15, no. 5, pp. 1477–1488, 2013.
- [19] R. Ortega, A. Loria, and P. Nicklasson, *Passivity-Based Control of Euler-Lagrange Systems: Mechanical, Electrical and Electromechanical Applications*, Springer, Berlin, Germany, 1998.
- [20] B. Gao, Y. Bao, J. Xie, and L. Jia, "Passivity-based control of two-dimensional translational oscillator with rotational actuator," *Transactions of the Institute of Measurement and Control*, vol. 36, pp. 185–190, 2014.